SSY186 - Image Reconstruction of Computed Tomography

Rita Laezza, Pavel Gueorguiev

April 2016

1 Introduction

Computed Tomography, commonly referred to as CT, is a method of combining X-ray images taken from multiple angles and using computer reconstruction algorithms for implementing a mathematical transform called the Radon transform. For the signal acquisition, X-rays are emitted from a source and the level of attenuation is recorded at the detector, after it passed through the object to be imaged. The detector usually contains: a collimator, scintillation crystals and photo-diodes, which together convert the X-ray energy into electrical signals. The signals are then input into the computer for signal processing.

The aim of this project is to explore different reconstruction methods, namely backprojection, filtered backprojection and convolution backprojection. Furthermore, a short section about fanbeam reconstruction is included. The underlying theory of the methods was presented and code was written to produce the necessary plots. All code was done using MATLAB.

2 Part A: Backprojection

The formulas (6.13) and (6.14) are used in the backprojection of the image.

$$b_\theta(x,y) = g(xcos(\theta) + ysin(\theta), \theta) \tag{1}$$

$$f_b(x,y) = \int_0^\pi b_\theta(x,y)d\theta \tag{2}$$

where $g(l,\theta)$ is the 2D Radon transform (a collection of line integrals through l at a certain angle θ). The numerical values physically represent the X-ray attenuation at the respective coordinates. The l variable consists of a parametric line in the plane which can be obtained using the following relation: $l = x \cdot cos(\theta) + y \cdot sin(\theta)$, where x and y are the coordinates of the backprojection image. An alternate name for $g(l,\theta)$ is a *sinogram*, due to objects appearing as collections of sine waves of varying amplitude and phase. As stated previously Equation 1 is simply assigning x and y coordinates according to the l projection. Figure 1 illustrates a backprojection of a sinogram at a 30° angle. Equation 2 is referred to as "backprojection summation". The principle behind this formula is that at a single angle θ there are an infinite number of objects that will give rise to the respective distribution. However, a summation over numerous angles will generate a unique image. It is made clear by equation 2 that only a range of 180° are needed to obtain a complete image. This is why the limits of the integration are from 0 to π.

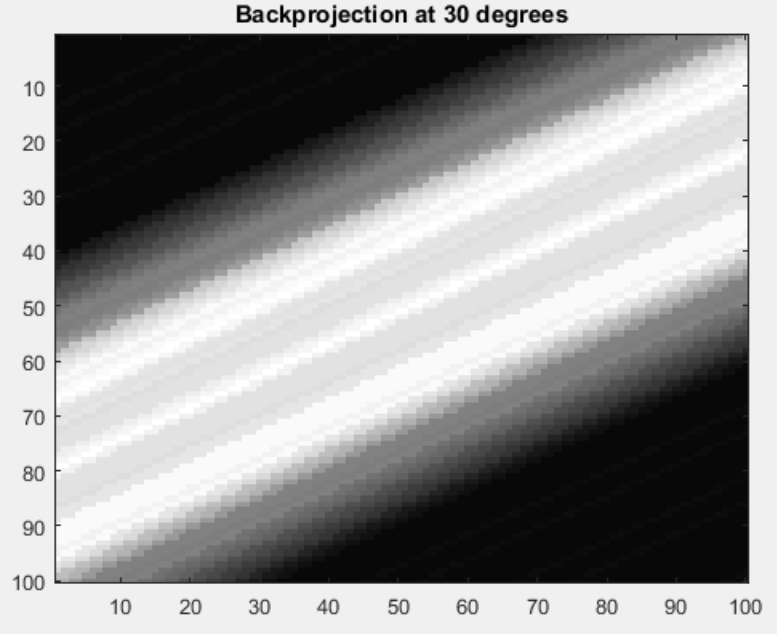

Figure 1: Backprojection of the sinogram data at $\theta = 30°$

In addition, the summation image has to be multiplied by a scaling factor $\pi/(2 \times N)$, where N is the number of backprojections added. The resulting image is sometimes called a *laminogram*. Figure 2 shows how the number of backprojections used for the reconstruction affect the quality of the image.

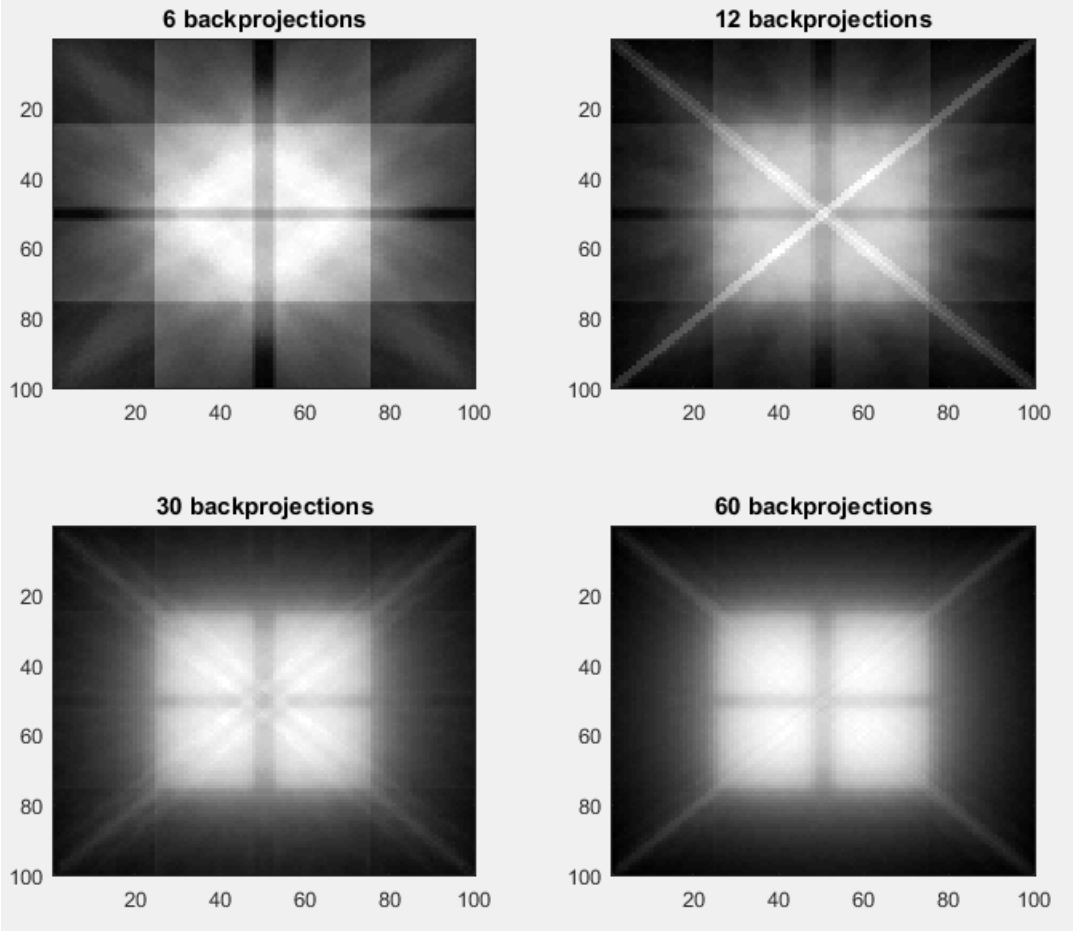

Figure 2: Backprojection summation images

Clearly, the more backprojections used, the more complete the reconstructed image becomes. Image 4 consists of the *laminogram* at all 180 different angles of the *sinogram*. However, adding the backprojections is merely a discrete approximation to the integral in figure 2. This will result in blurry images which is best explained as follows. From the projection-slice theorem (equation 6.18) it is understood that a projection at a certain angle corresponds to a line in the 2D frequency domain. Since we aren't sampling completely (non-continuum of angles) the low frequency components close to the centre will be sampled more than the high frequency (see figure 3), this creates an image that has the low frequency components overexposed, and hence its blurry appearance. In order to solve this issue a new procedure called Filtered Backprojection (FBP) was developed, which is thoroughly explained below.

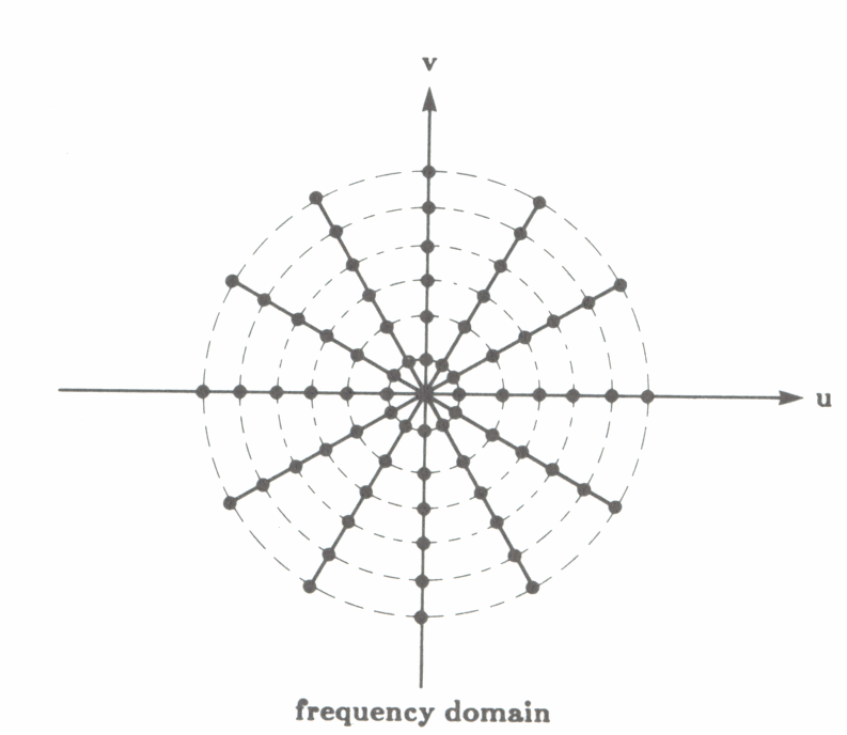

Figure 3: Illustration of the projection-slice theorem, object sampled at 6 discrete angles

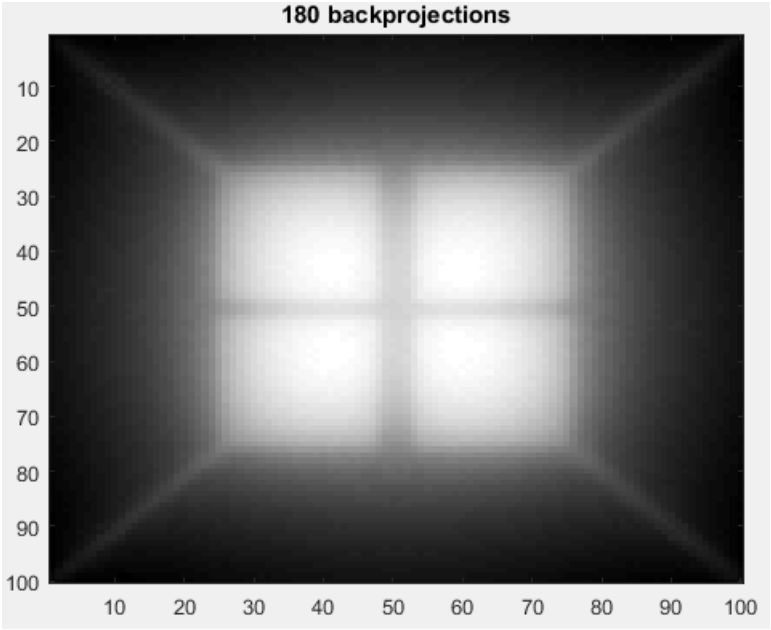

Figure 4: Summation image with 180 backprojections

3 Part B: Filtered Backprojection (FBP)

The flow chart in Figure 5 illustrates the steps necessary to compute the filtered backprojection. The first step is to compute the one-dimensional Fourier transform, $\mathcal{F}_l$, of the sinogram data, $g(l, \theta)$. The resulting signal, $G(\rho, \theta)$, is then filtered with a Ramp filter and subsequently inverse Fourier transformed to obtain $g_{filtered}(l, \theta)$. Finally, the reconstructed image is obtained by doing backprojection.

$$f(x,y) = \int_0^{\pi} \left[\int_{-\infty}^{\infty} |\rho| G(\rho,\theta) \exp^{j2\pi\rho l} \, d\rho \right]_{l=xcos\theta+ysin\theta} d\theta \tag{3}$$

The whole process can be expressed by equation 3. The inner integral corresponds to the 1D inverse Fourier transform with respect to ρ of $G(\rho, \theta)$. The term $|\rho|$ makes the equation a filtering operation. Finally, the outer integral consists of the backprojection summation.

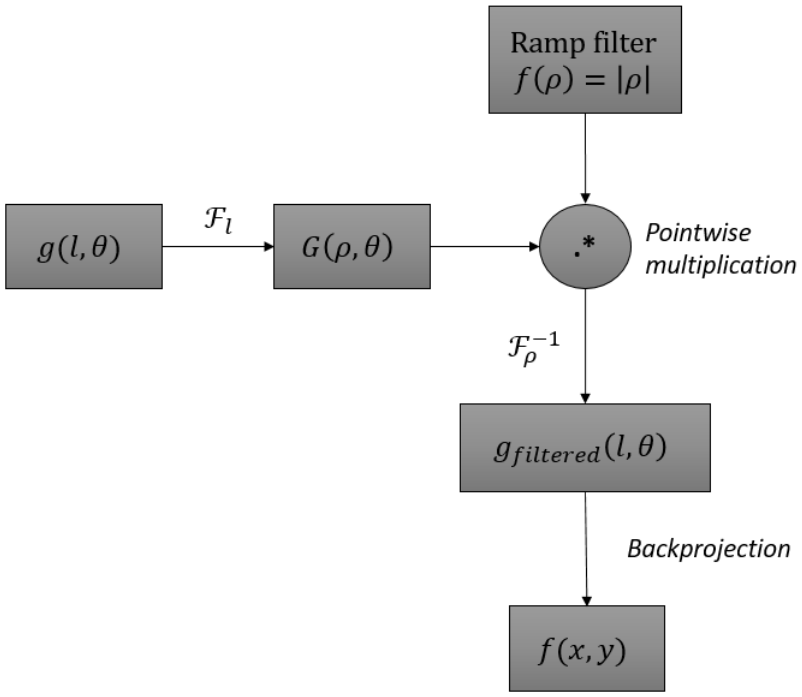

Figure 5: Flow chart

When comparing figure 4 with the two filtered results in figure 9 we can see that filtering improves substantially the blurriness of the reconstruction, as expected. In figure 6 the ramp filter is shown on the left. This is a very useful high pass filter for controlling the effects of the overexposed low frequency components. The filter on the right of figure 6 is the Hamming window that was multiplied with the ramp to obtain better results. A comparison of the two reconstructed images is shown in figure 9. The difference between simply using the ramp versus the combination of ramp and Hamming is described below.

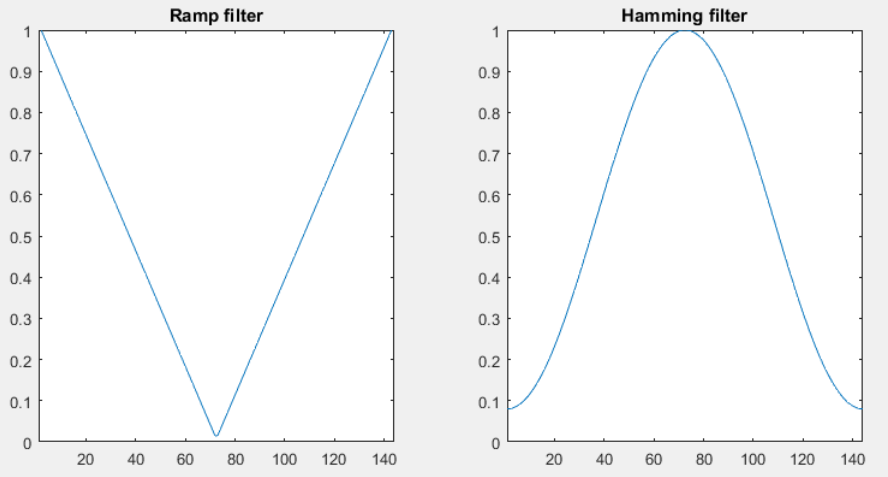

Figure 6: Diagram showing the ramp and Hamming filters side by side

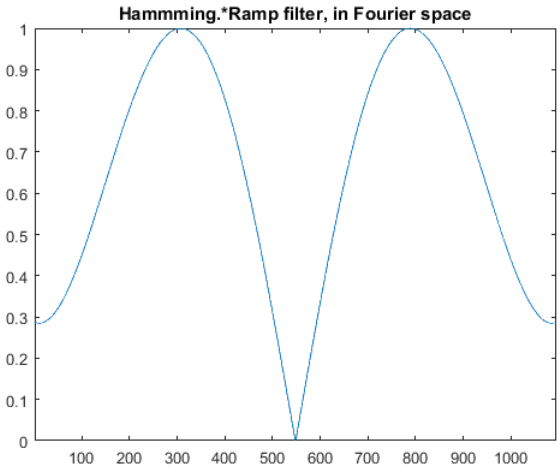

Figure 7: Diagram showing the combined ramp and Hamming filter used in Part E.

Similarly to part A, the more backprojections (N) used the better the reconstructed image becomes. This is clear for both the Hamming and the Ramp results. To obtain the best comparison between the two algorithms, we can look at figure 9 with 180 backprojections. Looking at the two images it is obvious that the bright area of the phantom does not appear as bright with the ramp filter. The constant coloured phantom is of low frequency and is getting filtered heavily by the ramp filter, since at the origin the filter approaches zero. The multiplication with the Hamming filter, on the other hand, possesses another property. While still filtering the low frequencies it also attenuates the very high frequencies, which usually only represent noise (static). The ramp filter in conjunction with a Hamming window produces a more truthful representation of the object. The resulting filter shape can be seen in figure 7. The advantage of applying a Hamming filter can be seen in figure 9. Clearly, the image on the right has far less noise than the one on the left.

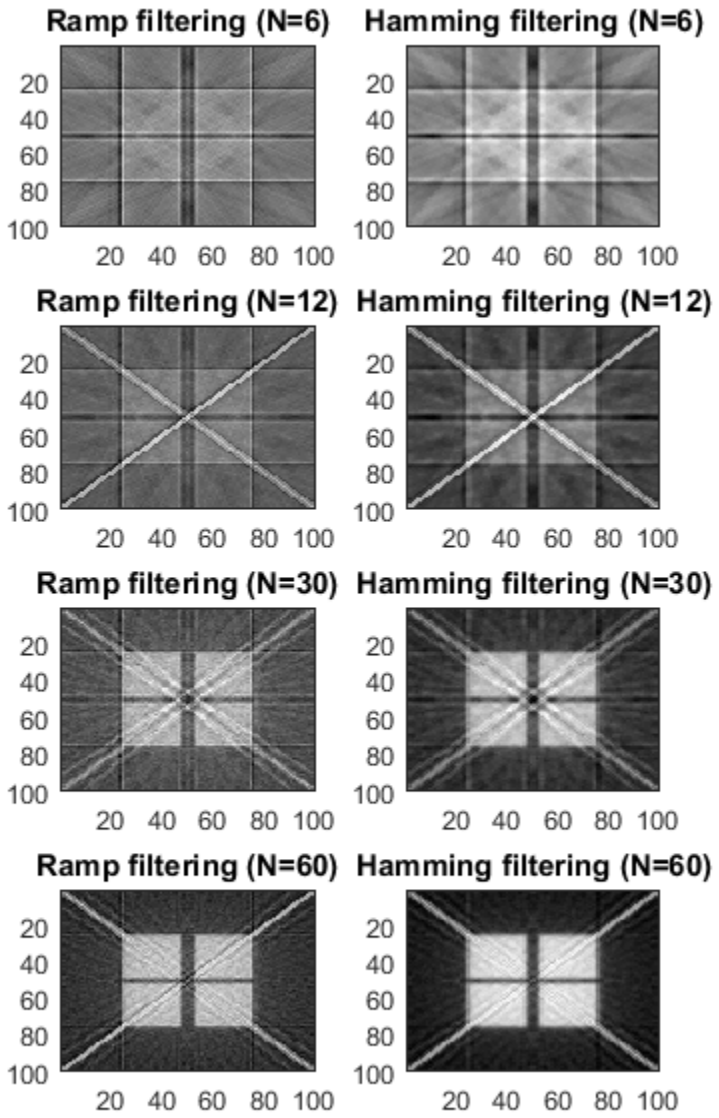

Figure 8: Summation images for Filtered Backprojection (Ramp vs Hamming windows)

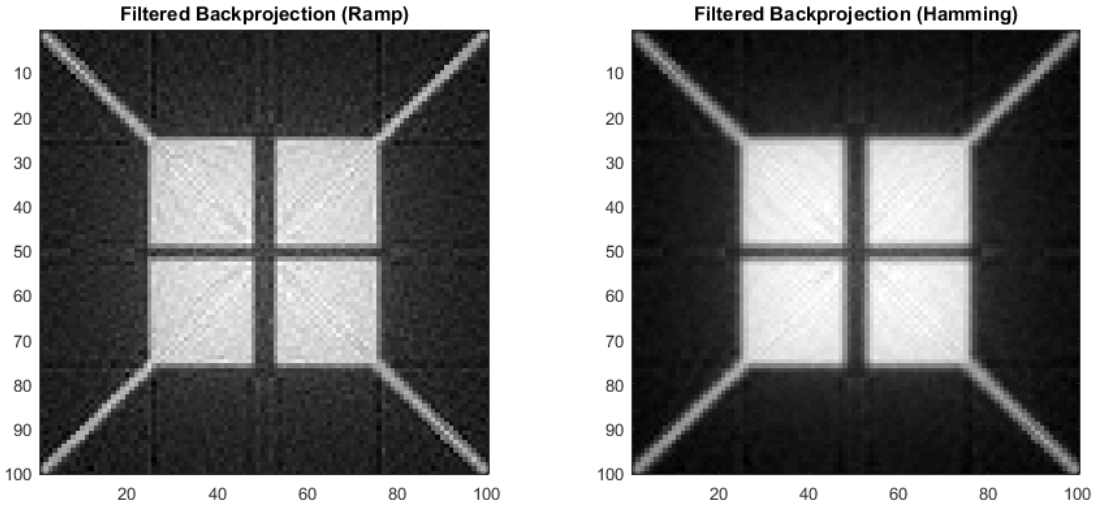

Figure 9: Filtered Backprojection for 180°

4 Part C: Convolution Backprojection (CBP)

The major difference between filtered backprojection and convolution backprojection approaches is that the filtering operation in FBP is implemented using a Fourier Transform while in CBP it is implemented using a convolution. Numerically the Fourier Transform is implemented using the Fast Fourier Transform (FFT) algorithm and is expected to be faster than convolution. Even though in theory the approaches lead to the exact same result, due to the implementation in the algorithms there will be small numerical deviations in the results. A comparison of the two approaches can be seen in figure 10.

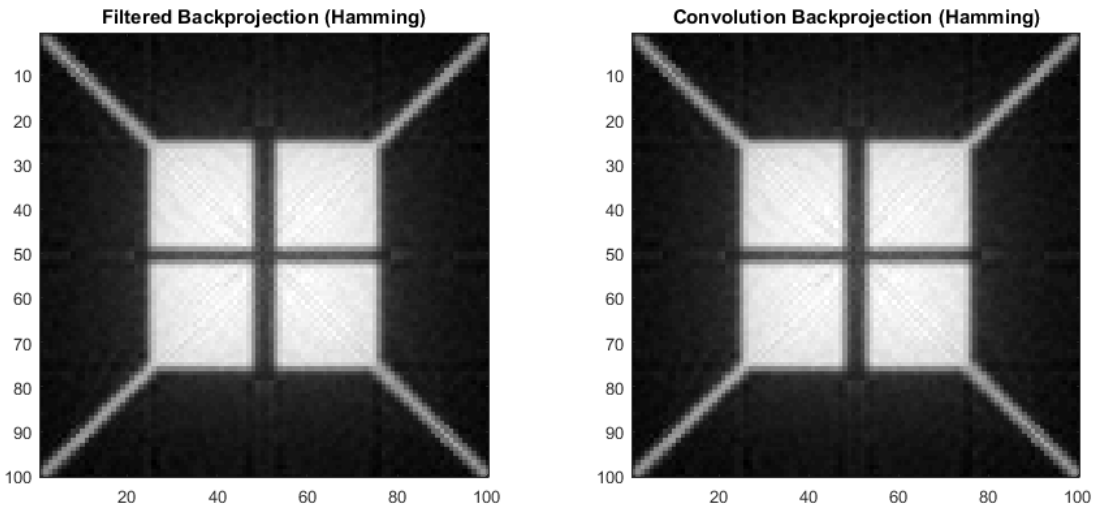

Figure 10: Filtered Backprojection vs Convolution Backprojection

In this case, the results are extremely similar with both the CBP and the FBP, using Hamming window. For that reason, the choice of method is only relevant for coding purposes, since the reconstruction results are visually equivalent.

5 Part D: Fan-Beam Projections

In the previous exercises the source was assumed to emit straight, parallel rays into the body and detected on a flat plate. Yet all modern CT scanners use a source that emits X-rays in a 'fan based' pattern, as well the detectors can be arranged in a semi-circular arc. The reconstruction cannot be the same as used in the previous sections and therefore requires modifications. The textbook explains a convolution backprojection algorithm for the third case described below.

The three basic geometries are as follows, and are also in figure 11:

1. Source X-rays have uniform angular spacing over the fan arc.
2. Detectors have uniform angular spacing (see figure 11, right side).
3. Both source X-rays and detectors have uniform angular spacing, here the detectors must be positioned on an arc (see figure 11, left side).

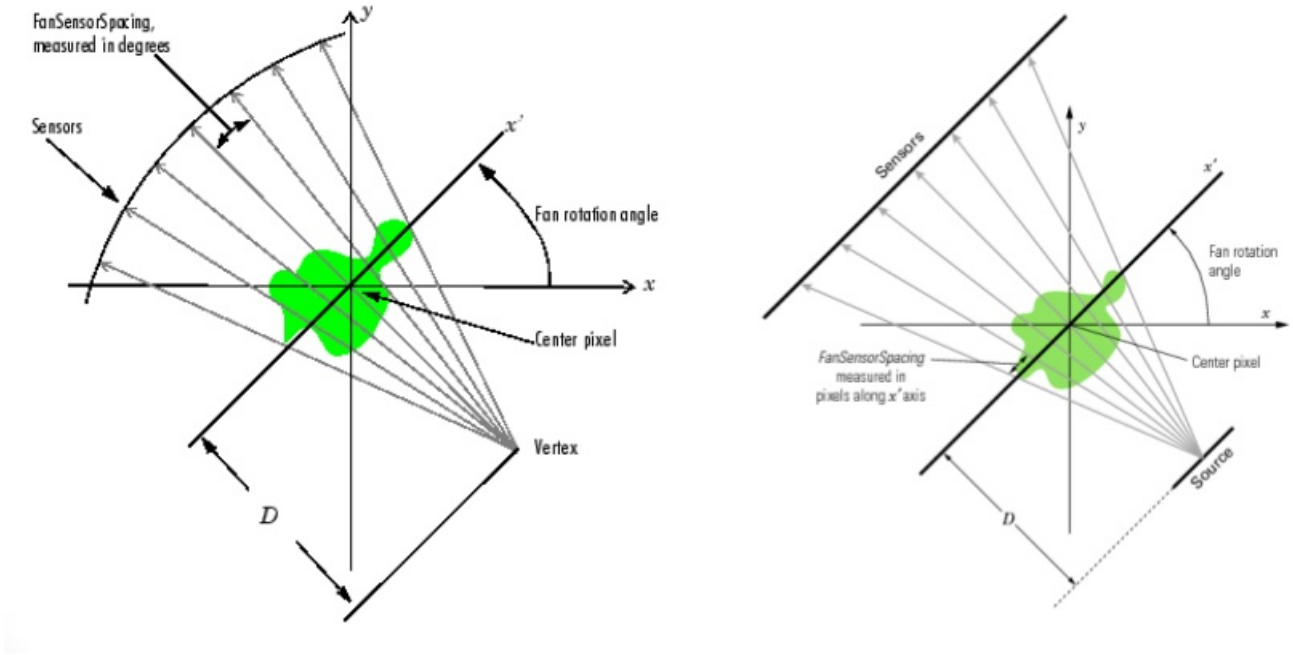

Figure 11: Geometries for fan-beam reconstruction

As stated previously the parallel derivation of the reconstruction techniques cannot be directly applied here, due to the different geometry of the source emitted rays. The coordinates describing the projections must be modified by using the following two transformations:

$$\theta = \beta + \gamma \tag{4}$$

$$l = Dsin(\gamma) \tag{5}$$

where D is defined as the distance from the source to the origin. Using the process used for parallel reconstruction and substituting the previously stated relations forms the first step of the derivation. The Jacobian of the following transformation ($Dcos\gamma$) and direct substitution will lead to:

$$f(r,\phi) = \frac{1}{2}\int_{-\gamma}^{2\pi-\gamma}\int_{sin^{-1}\frac{-T}{D}}^{sin^{-1}\frac{T}{D}} g(Dsin(\gamma),\beta+\gamma)\cdot c(rcos(\beta+\gamma-\phi)-Dsin(\gamma))Dcos(\gamma)d\gamma d\beta \tag{6}$$

This integral can be simplified with a few observations which will lead to the basic fan-beam reconstruction formula. The benefits of the fan-based image acquisition is: faster imaging speed at a cost of increased algorithm complexity.

6 Part E: Real CT-image

For this part we were given a second sinogram for which we had to adapt our algorithm due to the change in matrix dimensions. The image contains a source rotation of 180 degrees for 1095 parallel beams. Please refer to the MATLAB function 'backProjection2.m'.

Judging from figure 12 both the FPB and CPB provided better results than the simple backprojection algorithm. Looking closer at the fine details of the image, the FBP and CBP display the teeth with better resolution while in the backprojection the teeth appear blurry. From our timing results, advantage of the convolution methods with respect to the filtered is that it is slightly faster (this was unexpected since the FFT is a faster algorithm than conv). The algorithm improvements are in the Conclusion.

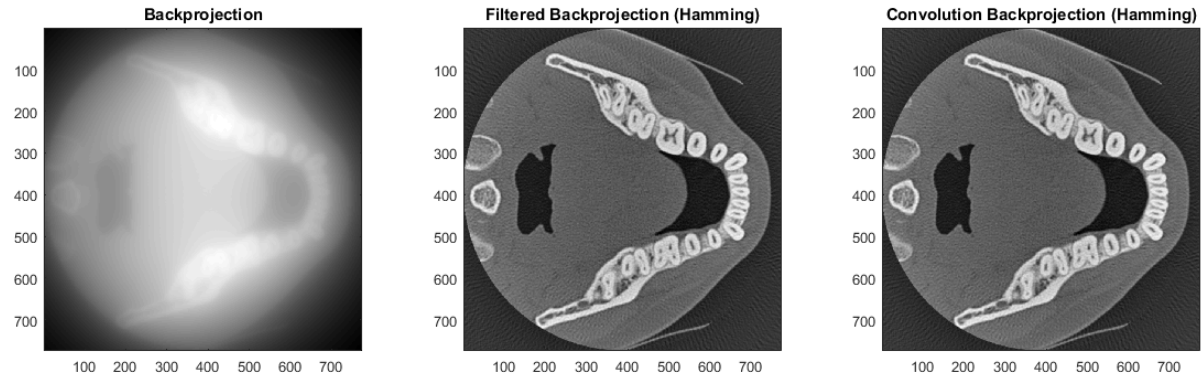

Figure 12: Reconstructed mandible using Backprojection, Filtered Backprojection (Hamming filter), and Convolution Backprojection (Hamming Filter)

7 Discussion

Some possible improvements for the filtered methods include implementing different filters for a more proportional frequency scaling while preserving some low frequency components (see figure 6.14 in p.200 of the textbook). Furthermore, post-processing can be done on the images to remove artifacts resulting from the backprojections. For this report we were given images collected at 180 degrees, however it is also possible to perform acquisition with more finely divided θ angles (as opposed to 1 degree in our project). According to the lecture material, the number of projections should be roughly the same as the number of rays in each projection, namely 1095.